



Cite this: *Chem. Commun.*, 2017, 53, 10244

## Escaping the trap of complication and complexity in multiscale microkinetic modelling of heterogeneous catalytic processes

Matteo Maestri 

In this feature article, the development of methods to enable a hierarchical multiscale approach to the microkinetic analysis of heterogeneous catalytic processes is reviewed. This methodology is an effective route to escape the trap of complication and complexity in multiscale microkinetic modelling. On the one hand, the complication of the problem is related to the fact that the observed catalyst functionality is inherently a multiscale property of the reacting system and its analysis requires bridging the phenomena at different time and length scales. On the other hand, the complexity of the problem derives from the system dimension of the chemical systems, which typically results in a number of elementary steps and species, that are beyond the limit of accessibility of present-day computational power even for the most efficient implementation of atomistic first-principles simulations. The main idea behind the hierarchical approach is to tackle the problem with methods of increasing accuracy in a dual feed-back loop between theory and experiments. The potential of the methodology is shown in the context of unravelling the WGS and r-WGS catalytic mechanisms on Rh catalysts. As a perspective, the extension to structure-dependent microkinetic modelling is discussed.

Received 24th July 2017,  
Accepted 17th August 2017

DOI: 10.1039/c7cc05740g

[rsc.li/chemcomm](http://rsc.li/chemcomm)

*Laboratory of Catalysis and Catalytic Processes, Dipartimento di Energia,  
Politecnico di Milano, via La Masa 34, 20156, Milano, Italy.  
E-mail: matteo.maestri@polimi.it*



Matteo Maestri

Matteo Maestri is Professor (associate) of Chemical Engineering at the Politecnico di Milano, Italy. He received the PhD *summa cum laude* in Chemical Engineering from the Politecnico di Milano in 2008 under the supervision of Prof. E. Tronconi. He has been visiting scholar at the Center for Catalytic Science and Technology of the Department of Chemical Engineering of the University of Delaware, USA (2006–2007) under the guidance of Prof.

D. G. Vlachos, and Alexander von Humboldt Fellow at the Fritz-Haber-Institut der Max-Planck-Gesellschaft in Berlin, Germany (2009–2010) and at the Catalysis Research Center (CRC)-Department of Chemistry of the Technische Universität München, Germany (2011) in the group of Prof. K. Reuter. His main research interests are fundamental analysis of catalytic kinetics and first-principles based multiscale modelling of gas–solid catalytic processes.

### 1. Introduction

At its fundamental nature, catalysis is a kinetic phenomenon.<sup>1</sup> Heterogeneous catalysts are functional materials with specific “active sites” which allow for the stabilization of the free energy of intermediates and transition states (TS) with respect to the relevant reactants, thus providing an enhancement of the rate of the overall reaction. If more than one reaction product is possible, the selectivity of such rate-enhancement towards specific steps of the network is a crucial task to favour the formation of particular products and it is at the basis of very important industrial processes.<sup>2,3</sup> This effect depends not only on the specific stabilization of free energies at the active site, but also on the chemical potential around it, which is determined by the reaction environment, in terms, *e.g.*, of composition, surface coverage, temperature and pressure. Thus, phenomena at very different time and length scales concur to establish the observed functionality of a catalyst material, as schematically reported in Fig. 1.<sup>4,5</sup> At the microscale, the kinetic parameters of the elementary steps are related to the making and breaking of chemical bonds and ultimately to the behaviour of the electrons and the interactions between the active site and molecules. At the meso-scale the rates of the possible elementary events and their interplay give rise to the prevalent catalytic mechanism. These phenomena are governed by the electronically determined microscopic parameters at the microscale under the specific



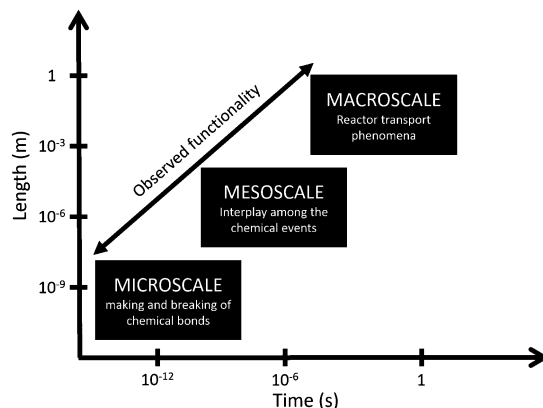


Fig. 1 Schematic representation of the time and length scales involved in a catalytic process. Adapted with permission from ref. 39.

conditions of pressure, temperature, and composition dictated by the transport and the hydrodynamics at the macroscale. As a result, different prevalent catalytic mechanisms can be established in response to the different conditions of the reaction environment. Hence, the macroscopic observed functionality of a given catalyst is an intrinsic multiscale property of the system. Therefore, the understanding of the macroscopic functionality of a catalyst requires addressing and linking the wide range of phenomena at the different time and length scales of Fig. 1.

Multiscale analysis based on microkinetic modelling is acknowledged to be the essential key-tool to contribute to this quest, thus providing fundamental insights into the functional-based understanding of a catalytic process.<sup>5</sup> Essential to this approach is the application of fundamental theoretical concepts for explaining the catalytic phenomenon, avoiding concepts that cannot be translated into theoretically accessible phenomena.<sup>6</sup> This implies, in particular, the separation of the overall reaction into individual elementary events and the use of electronic-structure theories and statistical thermodynamics to estimate their rate parameters.<sup>1,7</sup> The same approach also applies to the transport at the macroscale, by coupling the calculations of the rates of the elementary steps with a detailed modelling of the reaction environment.

The last decade experienced steadily growing progress in the way how predictive-quality theory and simulation can be quantitatively applied to address this task.<sup>8</sup> First-principles multiscale modelling is currently one of the most emerging and challenging topics in modelling catalysis. The possibility of modelling the surface chemistry in detail and at the fundamental level enables the consolidation of fundamental knowledge about a catalytic process under different operating conditions. Despite its attractive potential, the application is still strongly limited by the inherent complication and complexity of the problem, which make such an approach limited and prohibitive for most of the processes of technological interest.<sup>9</sup> On the one hand, the “complication” of the problem is related to both the accuracy of the methods employed at the different scales (e.g., the availability of exchange and correlation functionals able to predict the kinetic parameters within chemical accuracy

or accurate semi-empirical models) and the realization of a proper coupling of the phenomena at different time and length scales. The latter is very challenging even for model systems, because it is inherently rooted in the very different time and length scales to be bridged.<sup>10</sup> On the other hand, the “complexity” of the problem is related to the dimension of the problem especially at the microscale (e.g., the number of the elementary steps and species involved), which is very much beyond the limit of applicability of first-principles methods. Thus, the scientific community is in great need of methodologies to escape this “complication and complexity trap” in the multiscale microkinetic modelling of heterogeneous catalytic processes.

In this feature article, I will go over the path my research program took to address this challenge. In particular, I will first review the main causes of the intrinsic “complication” of the multiscale problem and I will present the methodologies for escaping this “complication” trap. Then, I will give an overview of the foundation and application of the hierarchical multiscale approach as a promising methodology for properly decoding the system complexity in the first-principles modelling and analysis of reaction mechanisms in heterogeneous catalysis. The potential of the approach will be illustrated by means of a show-case in the context of unravelling the reaction mechanism of WGS and r-WGS on Rh catalysts. Finally, I will give an overview of the main progress areas towards the full integration of first-principles analysis in multiscale modelling of heterogeneous catalysis by the development of structure-dependent microkinetic models.

## 2. Escaping the trap of complication

In this section, I will review the source of the complication in microkinetic multiscale modelling and the main developments to overcome this issue. The trap of complication of the multiscale problem refers both to the accurate description of the phenomena at the different scales and to the need of coupling them in a seamless simulation from atoms to the reaction environment. These aspects are intrinsically rooted in the nature of the multiscale problem, irrespective of the dimension of the system under consideration.<sup>10</sup>

### 2.1. Microscale

In the context of multiscale modelling, the term microscale refers to the estimation of the kinetic parameters (e.g., activation energy) of the elementary reactions. The calculation of these parameters is typically performed within the validity of the harmonic Transition State Theory (h-TST). In this context, the most important information for the determination of a rate constant is the location of the transition state of the different elementary steps at the catalytic surface.<sup>11</sup> Electronic structure theories, comprising *ab initio* quantum chemistry as well as density-functional methods (DFT), explicitly treat the electronic degrees of freedom and are the natural base for the calculation of the potential energy surface. DFT with semi-local (e.g., generalized gradient approximation, GGA) functionals is currently the most



used method among the electronic-structure theories.<sup>12–15</sup> On the one hand, such analysis can provide a detailed picture of the elementary reaction that is of direct use in kinetic studies. On the other hand, the uncertainty of the used exchange and correlation functional – with expected typical errors in DFT-GGA barriers of the order of ~0.2 eV – has to be always kept in mind, especially in the quest of a (semi-) quantitative prediction of the rates. A comprehensive review on the state-of-the-art use of electronic structure theory calculations in catalysis can be found in ref. 5 and 8.

Considering the huge computational cost connected to these calculations, semi-empirical and less demanding methods are typically used in microkinetic modelling, especially for the exploration of the complex reaction network.<sup>16</sup> Indeed, these methods, such as the Brønsted–Evans–Polanyi (BEP) relation or the unity bond index-quadratic exponential potential (UBI-QEP) method, can be very useful to get a first-screening of the activation energies of the reaction network or to account for coverage effects at negligible computational cost.<sup>17</sup> Typically, these methods allow for the calculation of activation energies only by means of thermochemical information of the species involved in the reaction. For instance, the UBI-QEP method is based on the assumption that in a many-body system the two-body interactions are described by a quadratic potential of an exponential function of the bond distance, called the bond index.<sup>18</sup> Then, the total energy of the many-body system is constructed from additive two-body contributions under the heuristic assumption that the total bond index of the system is conserved at unity. This leads to analytical expression for the total energy and eventually for the activation energy of an elementary step. With reference to Fig. 2, the activation barrier for a dissociating molecule turns out to be

$$\Delta E_{AB,original} = \phi(E_{TS} - Q_{AB} - D_{AB}) \quad (1)$$

which can be expressed as a function of thermochemical properties of the species involved in the reaction (the details of the derivation are given in ref. 18):

$$\Delta E_{AB,original} = \phi \left( D_{AB} + Q_{AB} - Q_A - Q_B + \frac{Q_A Q_B}{(Q_A + Q_B)} \right) \quad (2)$$

where  $D$  is the dissociation energy in the gas phase and  $Q$  are the binding energies of the species. The parameter  $\phi$  retains

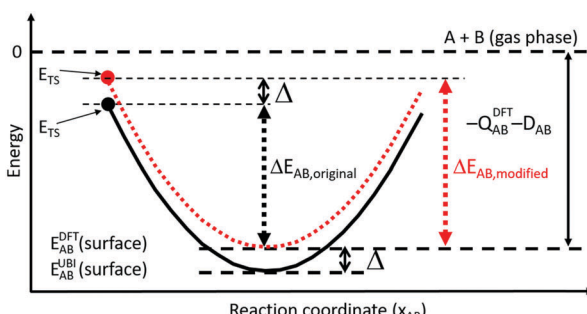


Fig. 2 Illustration of the UBI-QEP minimum energy path for a diatomic molecule AB interacting with a surface. Adapted with permission from ref. 23.

the information on the nature of the transition state. Given the impossibility of the semi-empirical method of locating the TS, the parameter is empirically set to 0.5, as an intermediate value between fully “early” ( $\phi = 0$ ) and fully “late” ( $\phi = 1$ ) TS. Thus, the UBI-QEP approach allows for the estimation/correlation of the reaction barriers on the basis of only one external parameter ( $\phi$ ) through eqn (2). This is different from the BEP relations, where two external parameters (the slope and the intercept) need to be determined. Typically, the values of the binding energies of the species involved are taken from methods and information which are different from the UBI-QEP (e.g., from DFT calculations or experiments) and the semi-empirical method is only used to provide an estimation of the reaction barrier. This is typically referred as the “hybrid UBI-QEP”.<sup>9,19,20</sup> On one side, these methods make tractable the microkinetic modelling of large reaction systems. On the other side, one must be aware of the accuracy of such semi-empirical methods, which are usually invalidated and dismissed as unreliable by the *ab initio* community.<sup>21,22</sup> In this respect, part of my research program has been devoted to the use of first-principles analysis to systematically validate and refine such semi-empirical methodologies. Next, I present the first-principles assessment and refinement of the UBI-QEP semi-empirical method.<sup>23</sup>

**2.1.1. First-principles assessment and refinement of the UBI-QEP method.** A systematic benchmark against first-principles data for a representative set of reactions has been performed to assess the limitations of the UBI-QEP and to identify strategies to overcome them. To this aim, an extensive DFT dataset for a range of surface catalytic reactions in the context of water–gas shift (WGS) and steam reforming (SR) of CH<sub>4</sub> at Rh(111) and Pt(111) surfaces at different values of surface coverage has been considered and compared to the UBI-QEP prediction.<sup>23</sup> The comparison is shown in Fig. 3. The dominant formulation of the UBI-QEP method was found to exhibit large errors, with individual barriers deviating by more than 100% from the reference DFT value. This apparent inconsistency turns out to be related first to the blindness of the hybrid UBI-QEP with respect to the nature of the TS of the reaction. In fact, considering the empirical choice of  $\phi$ , a first straightforward explanation for this discrepancy is that the empirical value  $\phi = 0.5$  does not account for the true nature of the TS. Insight into the nature of the TS needs to enter the scheme through the TS parameter  $\phi$ . Such insight is established for many classes of reactions or it can alternatively come from selected first-principles calculations. An additional issue is given by an intrinsic thermodynamic inconsistency when thermochemical data from various sources (e.g., DFT calculations or experimental data) are used in the hybrid UBI-QEP parameterization of eqn (2). In this situation, the binding energy from DFT does not coincide with the minimum of the UBI-QEP potential for the dissociating molecule. The difference between these two quantities (indicated with  $\Delta$  in Fig. 2) introduces an inconsistency between the energy of the TS from the UBI-QEP potential and the binding energy of the reactant molecule with respect to the zero-energy reference of Fig. 2. A simple corrective to this inconsistency is to simply shift the minimum energy path obtained with the UBI-QEP potential, so that its minimum



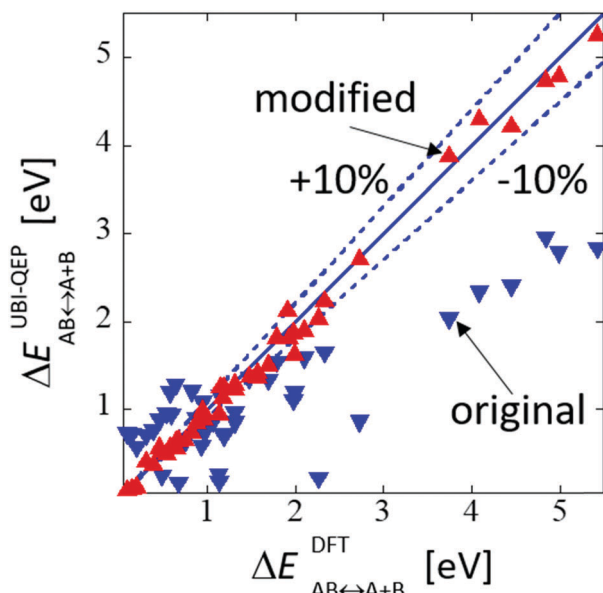


Fig. 3 Benchmark of UBI-QEP derived against DFT activation energies for various dissociation reactions at Rh(111) and Pt(111) surfaces and at different oxygen coverage. Adapted with permission from ref. 23.

coincides with the binding energy used in the parametrization. This is done by analytically minimizing  $E_{AB}^{M\!E\!P}$  and inserting the resulting expression in the equation for the activation energy:

$$\Delta E_{AB, \text{modified}} = \phi(E_{TS} - \min(E_{AB}^{M\!E\!P})) \quad (3)$$

The UBI-QEP barriers according to the new parameterization (eqn (3)) are within a window of  $\pm 10\%$  around the DFT reference data, as summarized in Fig. 3. As such, this semi-empirical estimate for the barriers can provide at controlled uncertainty most useful insights into complex reaction networks, where a full first-principles treatment is prohibitive. This modification has been discussed in detail in ref. 23 for the example of dissociation reactions, but is easily generalized to other classes of reactions.

## 2.2. Mesoscale

In the context of multiscale modelling of catalytic reactions, the term mesoscale typically refers to the calculation of the rates of the elementary events at the microscale. To this aim, the reaction is simulated as a rare event by coarse-graining the time evolution to the discrete rare event. This is governed by a Markovian master equation whose solution makes it possible to simulate time steps relevant to the reaction events.<sup>24–26</sup> The most common approach to the solution is the “mean-field” approximation, which relies on the assumption of very fast diffusion of the species at the surface. Under this assumption, the adsorbed surface concentration of each given species is considered equal everywhere at the surface, and thus the reaction rate of each elementary step can be expressed in terms of average surface coverage. In case the mean-field approximation cannot be considered valid, master equation based kinetic Monte Carlo (kMC) algorithms are employed in order

to account for the correct and site-resolved statistical interplay among the elementary steps of the microkinetic model.<sup>24,26</sup> The interplay among the rates of all the elementary steps at the microscale is crucial in determining the dominant paths, which take part in the catalytic cycle under given operating conditions. This is performed by reaction path analysis (RPA) based on the net-consumption rate of each species.<sup>9,20,27</sup>

## 2.3. Macroscale

The calculation of the rates at the mesoscale is performed for given values of the chemical potential (temperature, pressure, composition). Such values, however, change with time and space in the reactor and are governed by the transport phenomena at the macroscale. These transport phenomena are responsible for the macroscopic distribution of the velocity of the fluid (hydrodynamics), temperature, and composition, thus determining the reaction environment near the active site. The modelling of these phenomena is based on balance equations describing the conservation of mass, energy, and momentum.<sup>28</sup> The most advanced approaches are based on the computational solution of the momentum equation on a 3D geometry of the reactor *via* computational fluid dynamics (CFD) methods, which may include also the description of intra-particle transport phenomena.<sup>29–31</sup>

## 2.4. Bridging the scales

Besides the inherent complication related to the accurate description and estimation of the phenomena occurring at the different scales, an additional level of complication comes from the need of bridging the phenomena at the different characteristic scales.<sup>32</sup> This is crucial to the quest of deriving a mechanistic description of the catalyst functionality in working conditions. In this respect, a direct coupling is completely impractical from a numerical point of view, since it would require the bridging of more than twelve orders of magnitude along the time scale (Fig. 1). A computationally efficient formulation of the multiscale problem, instead, can be achieved by an effective decoupling of the interdependencies among the scales. The main feature of this approach is to treat each scale separately by introducing specific approximations to effectively decouple the characteristic time scales. In doing so, each scale is simulated with independent time steps, thus fully avoiding the direct coupling of phenomena occurring at very different characteristic times. Micro- and mesoscales are coupled by using either the mean-field approximation or the kMC method, that need eventually to be coupled with the description of the transport phenomena of mass, energy and momentum at the macroscale.

### 2.4.1. Coupling mean-field microkinetics and macroscale.

The mean-field approximation allows for a cost-free evaluation of the rate of each elementary reaction in terms of surface coverage. At a given value of surface coverage at the active site, one can directly calculate the corresponding reaction rates. Therefore, from a mathematical point of view, the coupling between mean-field microkinetic modelling and macroscale transport phenomena is controlled by the macroscale and the solution of the associated partial differential equation systems.



Peculiar to mean-field microkinetic modelling, however, is the need of a balance equation also for the adsorbed species, which is solved coupled with the gas phase mass balances. Contrary to what happens when a rate equation is employed, the number of gas and surface species, for which the mass balance must be solved, can be quite large and this may become a real numerical issue, especially when CFD is employed. Hence, the use of detailed microkinetic models in the framework of CFD simulations requires specific algorithms. In particular, the classical fully segregated approaches usually employed in most of non-reactive CFD simulations may result in strong numerical instabilities because of the combination of the stiffness of the elementary reactions with the typical large dimensions of a microkinetic model. In this context, the solution my group pursued is the application of the operator-splitting algorithm. When operator-splitting methods are employed, the governing equations are split into sub-equations. For the case of reacting flows in a catalytic reactor, the stiff and non-linear reaction operator is separated from the non-stiff and mildly non-linear transport term, thus making possible the solution of Navier-Stokes equations for complex and general geometries for reacting flows at surfaces, based on a detailed microkinetic description of the surface reactivity.<sup>29</sup>

**2.4.2. Coupling kMC and macroscale.** Contrary to mean-field microkinetic modelling, the inclusion of kMC simulations in the framework of reactor modelling requires the solution of the master equation, and thus the coupling between different time scales of the macroscale and mesoscale has to be realized. Thus, the calculation of the reaction rate at each time step and in each part of the domain of the reactor needs the explicit run of several kMC simulations for the estimation of the local reaction rates.<sup>33</sup> This dramatically limits the time step of the macroscale, thus resulting in unbearable computational costs. Key in this respect is the development of methodologies to minimize the number of kMC simulations that must be run “on the fly” during the simulation of the macroscale. To address this issue, we employed an instantaneous steady-state approximation to generically present the steady-state reactivity data in the form of an interpolated data field for the boundary condition.<sup>33,34</sup> This approximation exploits the typically different time scales of surface kinetics and macroscale transport phenomena. Upon a change of the local gas-phase conditions (temperature, pressure, concentrations), the surface relaxes to a new steady-state catalytic activity corresponding to these new conditions on time scales that are generally much shorter than those at which changes occur in the macroscopic fields. Hence, for any dynamical change of the flow field, the surface kinetics can thus be assumed to adapt instantaneously, and the reaction rates, at each time, are replaced by the steady-state reaction rates for the current gas-phase conditions. Under this approximation, it is sufficient to have a continuous representation of the steady-state reaction rates as a function of the gas-phase conditions. As such, the steady-state reaction rates can be pre-computed *via* kMC simulations independent of the reactor simulation. The kMC information is then used to determine a numerically efficient continuous representation by using either

tabulation techniques or suitable polynomial fits. Then, during the simulation, the species formation and consumption rates are evaluated by making use of the stored results, thus realizing a full decoupling among the interdependence of the characteristic times of meso- and macro-scale.<sup>33,34</sup> Despite its attractive potential, its applicability, however, has been so far proven only for systems with a limited number of elementary events and species (such as the CO oxidation on metal or oxide surfaces). Overall, these methodologies allow connecting a variety of models from *ab initio* calculations at the atomistic level to finite volume simulations at the macroscale. This provides an effective bridge between the intrinsic catalytic properties of the catalyst material when interacting with molecules of the surrounding gas phase and the macroscopic transport phenomena under the actual operating conditions, which, in turn, determines the local gas-phase concentrations and temperature at the catalyst surface.

### 3. Escaping the trap of complexity

In the previous section, I have shown the main developments in dealing with the intrinsic complication of the solution of the multiscale problem in heterogeneous catalysis. However, the application of the “first-principles” multiscale methodology to the system of technological relevance is also strongly hampered by the intrinsic complexity of the problems, *e.g.*, in terms of system dimension (*i.e.*, number of elementary steps, ...) or quantity of the information required for the application of the first-principles methods.<sup>10,35</sup> This complexity is particularly relevant at the microscale. For instance, the microkinetic model of a simple system such as partial oxidation of CH<sub>4</sub> on Rh is based on 41 reversible elementary steps between 13 adsorbed species.<sup>20,36,37</sup> The DFT-based computation of such a number of steps at different coverage would be a very demanding task and beyond the current computational capacity. This system complexity results in an effective limit which cannot be overcome by first-principles calculations (dashed line in Fig. 4).

The hierarchical multiscale approach, pioneered by Vlachos and co-workers,<sup>9,16</sup> is a very effective and promising methodology to escape the “complexity trap” in the first-principles analysis of heterogeneous catalytic processes. The approach is based on the premise that only certain events at each scale are, in practice, crucial for the accurate prediction of the macroscopic properties of the system. For instance, the dominant reaction mechanism under given operating conditions is the result of the interplay among all the possible and competing elementary steps at the microscale, but only a few of them will be part of the resulting dominant reaction mechanism. Therefore, instead of attempting to simulate all the possible chemical events with the highest accuracy, the full problem is tackled with an increasing level of complexity and computational cost to identify the main important and governing parameters, which are then further scrutinized by first-principles methods.<sup>36,38</sup> As such, first-principles methods are most effectively utilized, because there is detailed guidance as to what the most relevant issues are.



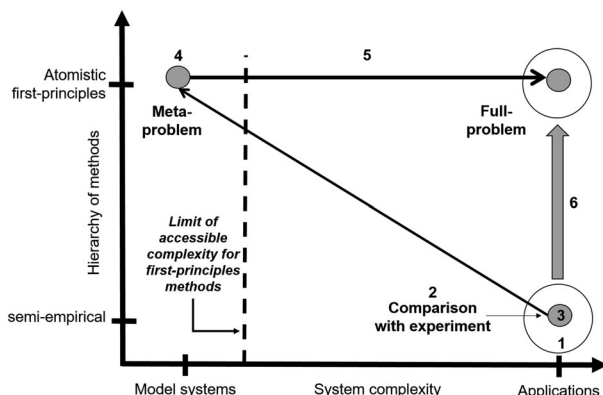


Fig. 4 Schematic representation of the hierarchical multiscale approach. Adapted with permission from ref. 36.

### 3.1. Foundation and description of the hierarchical approach

The main concept behind the hierarchical approach is to overcome the limit in the complexity accessible to first-principles methods by hierarchically applying methods of increasing accuracy and required computational time in a dual feed-back loop between theory and experiments. A general schematic of the hierarchical approach is summarized in Fig. 4. The procedure consists of the following general steps:<sup>9</sup>

(1) First the full problem is modelled by means of lower accuracy methods at affordable computational costs (point 1 in Fig. 4).

The semi-empirical model is then used for the analysis of a given experimental condition, and model results are compared with the selected experimental information (point 2 in Fig. 4).

(2) A detailed analysis of the inconsistencies between model results and experimental information is performed to relate them to specific parts of the model (shadowed circle, point 3 in Fig. 4). This is mostly done, for instance, by sensitivity analysis or mechanistic considerations, as shown later in Section 3.2.

(3) The so-identified sub-model (point 3) forms a meta-problem of reduced dimensions that can be refined with methods of higher accuracy, but computationally demanding (point 4 in Fig. 4). As a result, the hierarchical approach allows isolating from the full problem – which cannot be modelled directly with first-principles methods – a meta-problem of reduced dimension which is within the limit of the accessible complexity of first-principles calculations. In doing so, first-principles studies are focused on narrowly defined aspects and specific steps of the full model.

(4) The information obtained at the first-principles level is then back-input in the full problem (point 5 in Fig. 4), and, thus, an increase of the accuracy of the model is realized (point 6 in Fig. 4).

By sequentially analysing a comprehensive set of experimental conditions, the procedure permits the identification of different meta-problems. In doing so, the limit of the accessible complexity is overcome, and a hierarchical refinement of the full model is progressively realized.

In the specific context of unravelling the reaction mechanism of a catalytic process, the hierarchical approach encompasses the following steps.<sup>19,39</sup> First, an estimation of the kinetic

parameters of all the potential elementary reactions at the micro-scale is performed, using accurate but computationally non-demanding methodologies. These typically comprise semi-empirical theories such as the modified UBI-QEP method presented in Section 2.1.1. Then, the semi-empirical microkinetic model is used in conjunction with surface and reactor modelling in order to simulate the kinetic experiment. This allows for the calculation of the coverage of the adsorbates at the surface under the given operating conditions and for the identification of the dominant reaction mechanism *via* reaction path analysis (RPA) based on species net consumption rate.<sup>27,37</sup> The degree of rate control is then used to establish the rate determining step (RDS) of the catalytic cycle.<sup>40</sup> The comparison between model predictions and kinetic experimental information on the catalytic cycle (e.g., global reaction orders, RDS) is used for the identification of the key-features which need to be refined with first-principles methods. The parameters of the semi-empirical microkinetic model are adjusted on the basis of the insights derived from the first-principles calculations and the procedure is concluded when a full consistency between the predicted and experimental catalytic cycle is obtained for the specific set of experiments under examination. Next, I present a show-case of the application of the hierarchical multiscale methodology for the assessment of the catalytic mechanisms of WGS and r-WGS on Rh catalysts.

### 3.2. Show-case: unravelling the reaction mechanisms of WGS and r-WGS in Rh catalysts

Here, I review the application of the hierarchical multiscale approach for the unravelling of the catalytic mechanisms of WGS and r-WGS on Rh. The details of the methods are reported in ref. 38. The starting point of the analysis is the microkinetic model based on UBI-QEP methods reported in ref. 19 and the comprehensive set of WGS and r-WGS experiments in the annular reactor of Donazzi *et al.*<sup>41,42</sup> The experiments revealed first-order dependence with respect to  $\text{H}_2\text{O}$  and  $\text{CO}_2$  for the WGS and the r-WGS, respectively. This detailed microkinetic model includes several elementary steps for the WGS reaction such as redox, carboxyl (COOH) and formate (HCOO) mechanisms, as well as the direct oxidation of CO with OH species. These paths are summarized in Scheme 1.

Following the hierarchical multiscale approach, we first modelled the WGS and r-WGS experiments of Donazzi *et al.*,<sup>41,42</sup> using the UBI-QEP microkinetic model for the description of the microscale.<sup>19</sup> In each simulation, we considered the specific number of active sites as an independent input calculated from chemisorption experiments.<sup>19</sup> Fig. 5 shows the comparison between model prediction and experiments. The semi-empirical model underestimates the WGS and r-WGS at low temperature ( $<450^\circ\text{C}$ ). Then, at  $450^\circ\text{C}$ , a sharp increase in activity is predicted and the model suddenly reaches the equilibrium composition in contrast to what is experimentally observed. RPA is used to identify among the possible reaction steps the ones that are part of the dominant reaction mechanisms of WGS and r-WGS under the operating conditions of the experiments. The catalytic cycles derived *via* RPA are reported in Fig. 6.

$\text{CO}^* + \text{O}^* \leftrightarrow \text{CO}_2^* + \text{*}$	(s.1)
$\text{CO}^* + \text{OH}^* \leftrightarrow \text{CO}_2^* + \text{H}^*$	(s.2)
$\text{CO}^* + \text{OH}^* \leftrightarrow \text{COOH}^* + \text{*}$	(s.3)
$\text{CO}_2^* + \text{H}^* \leftrightarrow \text{COOH}^* + \text{*}$	(s.4)
$\text{CO}^* + \text{H}_2\text{O}^* \leftrightarrow \text{COOH}^* + \text{H}^*$	(s.5)
$\text{CO}_2^* + \text{OH}^* \leftrightarrow \text{COOH}^* + \text{O}^*$	(s.6)
$\text{CO}_2^* + \text{H}_2\text{O}^* \leftrightarrow \text{COOH}^* + \text{OH}^*$	(s.7)
$\text{CO}_2^* + \text{H}^* \leftrightarrow \text{HCOO}^{**}$	(s.8)
$\text{CO}_2^* + \text{OH}^* + \text{*} \leftrightarrow \text{HCOO}^{**} + \text{O}^*$	(s.9)
$\text{CO}_2^* + \text{H}_2\text{O}^* + \text{*} \leftrightarrow \text{HCOO}^{**} + \text{OH}^*$	(s.10)
$\text{H}_2\text{O}^* + \text{*} \leftrightarrow \text{OH}^* + \text{H}^*$	(s.11)
$\text{CO}^* \leftrightarrow \text{CO}^*$	(s.12)
$\text{CO}_2^* \leftrightarrow \text{CO}_2^*$	(s.13)
$\text{H}_2\text{O} + \text{*} \leftrightarrow \text{H}_2\text{O}^*$	(s.14)
$\text{H}_2 + 2\text{*} \leftrightarrow 2\text{H}^*$	(s.15)

Scheme 1 Possible elementary steps involved in the WGS and r-WGS reacting system and included in the semi-empirical microkinetic model.<sup>19</sup>

RPA based on the semi-empirical microkinetic model predicts that, for the WGS system (Fig. 6, panel a), first  $\text{H}_2\text{O}$  adsorbs at the surface and dissociates to OH and H. Then, CO, upon adsorption, converts to  $\text{CO}_2$  through direct oxidation by means of OH. According to the degree of rate control analysis,<sup>40</sup>  $\text{H}_2\text{O}$  dissociation turns out to be the RDS of the catalytic cycle, while all the other dominant steps are found to be partially equilibrated. Thus, the rate of WGS can be expressed as

$$r_{\text{WGS}} = \vec{k}_{11} \theta_{\text{H}_2\text{O}} \theta_{\text{Rh}} = \frac{\vec{k}_{14}}{\vec{k}_{14}} \vec{k}_{11} p_{\text{H}_2\text{O}} \theta_{\text{Rh}}^2 \approx \frac{\vec{k}_{14}}{\vec{k}_{14}} \vec{k}_{11} p_{\text{H}_2\text{O}} \quad (4)$$

For temperatures higher than 450 °C, the surface turns out to be mostly free (free sites >70%) and the above expression (eqn (4)) has been approximated for  $\theta_{\text{Rh}} = 1$ . This leads to a first-order macroscopic reaction order with respect to water and a zero-order with respect to CO, in agreement with the experimental evidence reported in ref. 42.

For the r-WGS system (Fig. 6, panel b), RPA indicates that the same elementary steps of the WGS (in the reverse way) are present in the catalytic cycle.  $\text{CO}_2$  reacts with H to give CO and OH and the RDS is identified as the water formation reaction ( $\text{OH} + \text{H} \rightarrow \text{H}_2\text{O}$ ). Thus, the resulting rate equation exhibits dependence on  $\text{H}_2$  which is at variance with the experimental information of first order dependence with respect to  $\text{CO}_2$  and zero-order with respect to  $\text{H}_2$  for r-WGS. In order to investigate the reasons behind this disagreement, we refined the identified dominant pathways (Fig. 6, panels a and b) through explicit DFT-PBE calculations. The first-principles refinement revealed that the direct oxidation of CO by OH ( $\text{CO} + \text{OH} \rightarrow \text{CO}_2 + \text{H}$  – step s.2 in Scheme 1) is not an elementary step. Thus, it cannot be considered as an alternative route to the carboxyl mechanism (steps from s.3 to s.10 in Scheme 1).<sup>36,38</sup> In fact, the identification of the minimum energy path (MEP) between reactants and products shows the pathway to proceed through the formation of different stable reaction intermediates. First, a *cis*-carboxyl ( $\text{COOH}$ ) forms. Then, the *cis*-carboxyl isomerizes to *trans*-carboxyl, before decomposing to  $\text{CO}_2$  and H. This peculiar insight is only achieved thanks to the first-principles analysis, as the semi-empirical UBI-QEP method cannot predict in any way the topology of the potential energy surface. Thus, it cannot differentiate whether a reaction step is elementary or not. Following the results from the first-principles analysis,

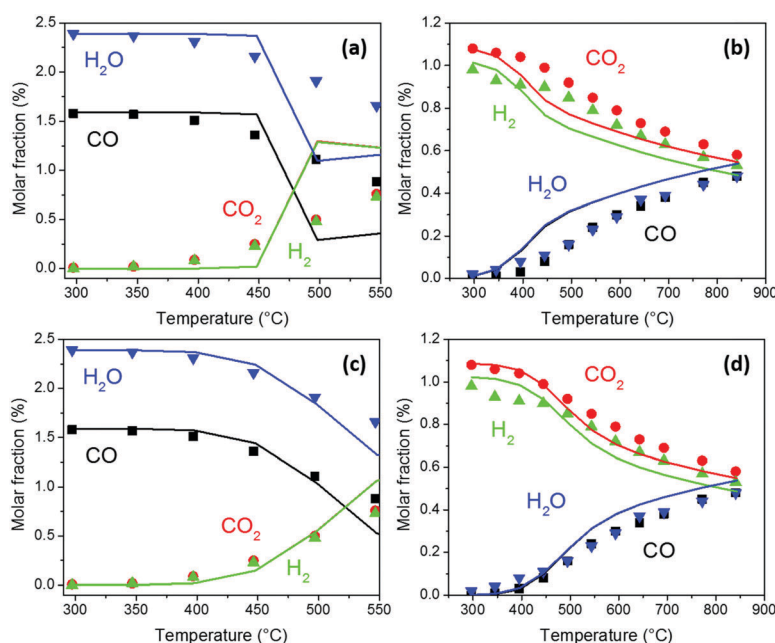


Fig. 5 Comparison between microkinetic model predictions (solid lines) and experimental data (symbols). Panel a: WGS, semi-empirical microkinetic model; panel b: r-WGS, semi-empirical microkinetic model; panel c: WGS, DFT-refined microkinetic model; panel d: r-WGS, DFT-refined microkinetic model. The details of the operating conditions are given in ref. 36. Adapted with permission from ref. 36.



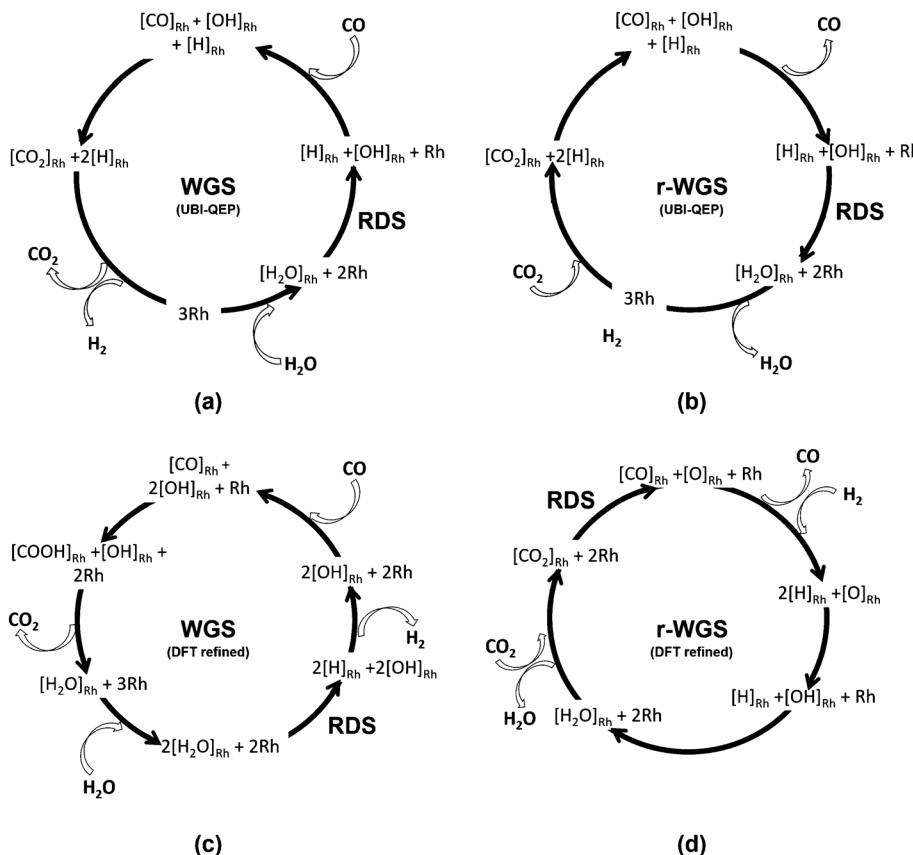


Fig. 6 Dominant reaction mechanisms for WGS and r-WGS on Rh. (a and b) UBI-QEP semi-empirical microkinetic model; (c and d) DFT-refined microkinetic model. Adapted with permission from ref. 38.

we removed this non-elementary step from the full microkinetic model and the parameters of the remaining reactions were fine-tuned in order to improve the quantitative prediction of the experiments (Fig. 5, panels c and d). It is worth stressing that the refinement cannot be achieved by the direct incorporation of the DFT energetics in the whole model because it would lead to completely unreliable results. In fact, the parameters of the elementary steps of the microkinetic model are not optimized *per se*, but with respect to the complete set of elementary steps forming the microkinetic model. Therefore, the refinement consists of translating the insights from the first-principles analysis into an educated modification of the parameters of the semi-empirical method (e.g., nature of the transition state *via* the  $\phi$  parameter, value of the pre-exponential factor, . . .). In this way, a DFT-refined microkinetic model is obtained. Besides the improved quantitative agreement, we also perform RPA based on the DFT-refined model in order to check the consistency with respect to the global reaction orders.

RPA revealed that WGS and r-WGS are now characterized by two different dominant reaction mechanisms under the investigated experimental conditions. Specifically (Fig. 6, panels c and d), for WGS conditions, water activation is the RDS and CO converts to  $\text{CO}_2$  through a carboxyl pathway. Since all the steps in Fig. 6 (panel c) except for the RDS turn out to be at partial equilibrium, still the observed reaction rate is given by eqn (4),

in agreement with the experimentally observed reaction order. For r-WGS, instead (Fig. 6, panel d),  $\text{CO}_2$  converts to CO *via* decomposition to CO and O. In this situation,  $\text{CO}_2$  decomposition turns out to be the RDS with all the other steps quasi-equilibrated. Thus, the rate of r-WGS (approximated for  $\theta_{\text{Rh}} = 1$  as done for eqn (4)) is now given by

$$r_{\text{r-WGS}} = \bar{k}_1 \theta_{\text{CO}_2} \theta_{\text{Rh}} = \frac{\bar{k}_{13} \bar{k}_1 p_{\text{CO}_2} \theta_{\text{Rh}}^2}{\bar{k}_{13}} \approx \frac{\bar{k}_{13} \bar{k}_1 p_{\text{CO}_2}}{\bar{k}_{13}} \quad (5)$$

Hence, the hierarchical refinement has led to first-order kinetic dependence on  $\text{CO}_2$  for r-WGS, thus reconciling the model predictions with the experimental findings. It is important to note that the prediction of having two distinct catalytic cycles for WGS and r-WGS is not in contrast with the microscopic reversibility. In fact, the experimental data herein analysed are in kinetically relevant conditions and thus far from thermodynamic equilibrium. In particular, in Fig. 5, temperature, but not surface and gas phase concentrations, is the same for forward (WGS) and reverse (r-WGS) reactions and indeed different concentrations of surface intermediates lead to different kinetic relevant steps in the two directions. By approaching equilibrium (e.g.,  $>650$  °C), instead, microscopic reversibility applies, and both the WGS and r-WGS reach the same equilibrium surface composition and the same elementary steps are present in both the catalytic cycles.<sup>36</sup>

Besides WGS and r-WGS, the hierarchical multiscale approach has been successfully applied for the microkinetic analysis of several reacting systems such as CH<sub>4</sub> steam and dry reforming and catalytic partial oxidation on Rh based catalysts.<sup>27,37,43,44</sup> These findings have been of direct use for the design and scale-up of short-contact-time reformers for small scale hydrogen production in the sustainable energy field.<sup>45</sup>

## 4. Conclusions and outlook

In this feature article, I have shown the main developments of my research program in the field of multiscale microkinetic modelling of catalytic processes. This is a very important task in the quest of achieving a functional based understanding of a catalytic material. Its application is strongly limited by the inherent “complication” and “complexity” of the problem. The hierarchical multiscale approach has demonstrated the potential of making it possible to escape these traps. The methodology is based on the use of methods of increasing accuracy (from semi-empirical methods to first-principles calculations) in a dual feed-back loop between theory and experiments. On one side, semi-empirical methods can effectively be employed in conjunction with first-principles studies for the exploration of complex reaction networks. On the other side, the complementary information from both theory and experiments allows for filling the gap to complexity and practical performances and for correlating the macroscopic observations to mechanistic insights. A successful application on the analysis of the reaction mechanism of WGS and r-WGS has been presented. This analysis has substantially contributed to the comprehension of the molecular level mechanisms underlying the complex experimental evidence in terms of macroscopic observed phenomena. Next, I will discuss the extension of the methodology to the inclusion of the catalyst structure under reaction conditions as the main direction in the attempt of achieving an atomistic level description of the catalyst functionality.

### 4.1. Beyond the concept of “static active site”

On the one hand, the hierarchical approach to multiscale modelling of catalytic processes has been shown to be very powerful in rationalizing the macroscopic kinetic features of the system. On the other hand, the rigorous understanding of the catalyst functionality at the atomistic level is still prevented by the strong approximations in the description of the active site.<sup>2</sup> In fact, even though the surface structure has been a key factor in catalysis science since the discovery of structure sensitive reactions in single crystal studies,<sup>46</sup> the effect of the structure of the catalyst on reactivity and selectivity is at present neglected in state-of-the-art microkinetic modelling.<sup>19,47–49</sup> This is mainly due to the enormous complexity associated with the accounting for the nature and the structural dynamics of the active site under given local operating conditions in the reactor. As such, these models rely on an abstract and static concept of the “catalyst material”, which is often modelled as a generic free site “\*” at the catalyst surface, without accounting for the effect of the

actual orientation and positioning of the atoms at the surface. Thus, this oversimplified model of the catalyst material creates a “material gap” in microkinetic modelling, which is also strongly impeding the quantitative implementation of atomistic first-principles kinetic analysis in the context of heterogeneous catalytic reaction modelling.<sup>21</sup> This was quite apparent in the show-case given in Section 3, where the information from the first-principles refinement was not used directly in the model, but was input *via* an educated modification of the parameters of the underlying UBI-QEP model.

At present, this situation impedes the rational and detailed interpretation of the structure–activity relation driven by fundamentals, which represents without doubts a crucial step toward the functional based understanding and design of a catalytic process. The need of accounting for the explicit effect of the active site in multiscale simulations of catalytic processes has a strong impact on both the inherent complication and complexity of the problem. As an example, in the case of metal supported nanoparticles, methods for the prediction of size and shape of the nanoparticle as a function of the chemical potential in the reactor are required.<sup>9,10</sup> Moreover, the necessity of building first-principles kinetic models not only for one facet, but for several ones, potentially including corners, edges, and defects, results in an explosion of complexity well beyond the limit of accessibility of present-day computational power even for the most efficient implementation of atomistic first-principles simulations. To this aim, the hierarchical multiscale approach represents an effective, but elegant manner to tackle this problem. Although its formulation remains fully equivalent in its essence to the description given in Section 3, novel methodologies and experimental techniques are needed. For instance, the prediction of the shape and size of the nanoparticle in reacting conditions calls for the validation of modified Wulff construction methods and kinetic growth models of the nanoparticle in multiscale simulations.<sup>50</sup> Moreover, the assessment and the validation of semi-empirical methods are needed to provide a proper parametrization of the kinetics on the different facets of the nanoparticle to enable the hierarchical approach for structure-dependent microkinetic modelling.<sup>51,52</sup> As an example, preliminary results from my group show that the nature of the TS is crucial in the application of UBI-QEP and BEP relations on different surfaces.<sup>53</sup>

Moreover, experimental information is a key aspect of the implementation of the hierarchical approach because it allows for filling the gap to complexity and practical performances by the identification of a meta-problem. Aiming at describing structural effects, it will be important to provide accurate and relevant spectroscopic and kinetic information under conditions of temperature, pressure and composition significant to catalysis. This calls for the design and development of novel tools of investigation that permit a concomitant and relevant collection of spectroscopic and kinetically relevant data. In this respect, my group recently presented a novel experimental tool that integrates *in situ* Raman spectroscopy and annular reactor for the operando-Raman kinetic analysis of heterogeneous catalytic reactions.<sup>54</sup> This reactor allows for detailed structural



characterization of a catalyst material during the reaction and under conditions of temperature, pressure and composition relevant to catalysis. Therefore, it is an important breakthrough for the simultaneous collection of spectroscopic and kinetically relevant data for the investigation of the structure–activity relationship in heterogeneous catalysis. The design and development of this innovative experimental tool has been performed by minimizing the mutual invasiveness of the Raman spectroscopy and of the annular reactor configurations. We demonstrate that the final configuration can monitor by Raman spectroscopy the catalytic surface under kinetically limited reaction conditions, with reliable product analysis, thus retaining the major features of both Raman spectroscopy and kinetic investigation in the annular reactor. These methodologies need to be coupled to microscopy information, in order to allow elucidation of working structures of catalysts, thus ultimately facilitating the development of models that capture active site characteristics.<sup>55–57</sup>

On a more general basis, structure dependent microkinetic modelling will enable the development of multi-site microkinetic models, which also include the effect of the support or defect sites, dynamics of catalyst nanoparticles with the changing reaction environment and size effects. Multiscale analysis of kinetic experiments by means of such envisioned microkinetic models will allow for the identification of catalyst descriptors based on a rigorous representation both of the catalyst functionality and of the catalytic cycle, and will be of direct use for the computational screening of different catalyst materials, thus providing guidelines for the design of new materials. As such, the envisioned extension of the hierarchical multiscale approach to the description of the active site will constitute a relevant change of paradigm in the analysis and design of complex catalytic processes, by paving the way towards a rational development based on functional understanding rather than empirical testing.

## Conflicts of interest

There are no conflicts to declare.

## Acknowledgements

I am grateful to my mentors, students and co-workers, past and present, for the stimulating collaborations and enlightening discussions. I am also thankful to various members of the catalysis community for valuable conversations and constructive criticisms on the development of the work herein reviewed in peer-reviews and conferences. I gratefully acknowledge the financial support over the years by the Alexander von Humboldt Foundation (Germany), the Italian Ministry of Education and Research (MIUR, Call SIR 2014 – Project THEOREMA – Grant RBSI14TG3E) and the European Research Council (ERC Starting Grant 2015 – Project SHAPE – Grant 677423).

## References

- 1 M. Boudart, *Catal. Lett.*, 2000, **65**, 1–3.
- 2 R. Schlogl, *Angew. Chem., Int. Ed.*, 2015, **54**, 3465–3520.
- 3 D. C. Tranca, N. Hansen, J. A. Swisher, B. Smit and F. J. Keil, *J. Phys. Chem. C*, 2012, **116**, 23408–23417.
- 4 K. Reuter, C. Stampfl and M. Scheffler, in *Handbook of Materials Modeling, Part A. Methods*, ed. S. Yip, Springer, Berlin, 2005, pp. 149–194.
- 5 M. K. Sabbe, M. F. Reyniers and K. Reuter, *Catal. Sci. Technol.*, 2012, **2**, 2010–2024.
- 6 R. Schlogl, *CATTECH*, 2001, **5**, 146–170.
- 7 J. A. Dumesic, G. W. Huber and M. Boudart, in *Handbook of Heterogeneous Catalysis*, ed. G. Ertl, H. Knozinger, F. Schuth and J. Weitkamp, Wiley-VCH, New York, 2008, vol. 3.
- 8 K. Reuter, *Catal. Lett.*, 2016, **146**, 541–563.
- 9 M. Salciccioli, M. Stamatakis, S. Caratzoulas and D. G. Vlachos, *Chem. Eng. Sci.*, 2011, **66**, 4319–4355.
- 10 M. Stamatakis, *J. Phys.: Condens. Matter*, 2015, **27**, 28.
- 11 D. Sheppard, R. Terrell and G. Henkelman, *J. Chem. Phys.*, 2008, **128**, 134106.
- 12 A. A. Gokhale, J. A. Dumesic and M. Mavrikakis, *J. Am. Chem. Soc.*, 2008, **130**, 1402–1414.
- 13 A. A. Gokhale, S. Kandoi, J. P. Greeley, M. Mavrikakis and J. A. Dumesic, *Chem. Eng. Sci.*, 2004, **59**, 4679–4691.
- 14 L. C. Grabow, A. A. Gokhale, S. T. Evans, J. A. Dumesic and M. Mavrikakis, *J. Phys. Chem. C*, 2008, **112**, 4608–4617.
- 15 J. Scarant and M. Mavrikakis, *Surf. Sci.*, 2016, **648**, 201–211.
- 16 J. E. Sutton and D. G. Vlachos, *Chem. Eng. Sci.*, 2015, **121**, 190–199.
- 17 R. A. Van Santen and M. Neurock, *Catal. Rev.: Sci. Eng.*, 1995, **37**, 557–698.
- 18 E. Shustorovich and H. Sellers, *Surf. Sci. Rep.*, 1998, **31**, 5–119.
- 19 M. Maestri, D. G. Vlachos, A. Beretta, G. Groppi and E. Tronconi, *AIChE J.*, 2009, **55**, 993–1008.
- 20 A. B. Mhadeshwar and D. G. Vlachos, *Combust. Flame*, 2005, **142**, 289–298.
- 21 J. E. Sutton, W. Guo, M. A. Katsoulakis and D. G. Vlachos, *Nat. Chem.*, 2016, **8**, 331–337.
- 22 J. E. Sutton and D. G. Vlachos, *J. Catal.*, 2016, **338**, 273–283.
- 23 M. Maestri and K. Reuter, *Angew. Chem., Int. Ed.*, 2011, **50**, 1194–1197.
- 24 K. Reuter, in *Modeling Heterogeneous Catalytic Reactions: From the Molecular Process to the Technical System*, ed. O. Deutschmann, Wiley-VCH, Weinheim, 2009.
- 25 B. Temel, H. Meskine, K. Reuter, M. Scheffler and H. Metiu, *J. Chem. Phys.*, 2007, **126**, 204711.
- 26 M. Stamatakis and D. G. Vlachos, *ACS Catal.*, 2012, **2**, 2648–2663.
- 27 M. Maestri, D. G. Vlachos, A. Beretta, G. Groppi and E. Tronconi, *J. Catal.*, 2008, **259**, 211–222.
- 28 R. B. Bird, W. E. Stewart and E. N. Lightfoot, *Transport Phenomena*, J. Wiley, New York, 2nd edn, 2002.
- 29 M. Maestri and A. Cuoci, *Chem. Eng. Sci.*, 2013, **96**, 106–117.
- 30 *Modeling of Heterogeneous Catalytic Reactions: From the Molecular Process to the Technical System*, ed. O. Deutschmann, Wiley-VCH, Weinheim, 2011.
- 31 T. Maffei, G. Gentile, S. Rebughini, M. Bracconi, F. Manelli, S. Lipp, A. Cuoci and M. Maestri, *Chem. Eng. J.*, 2016, **283**, 1392–1404.
- 32 F. J. Keil, *Comput. Math. Appl.*, 2013, **65**, 1674–1697.
- 33 S. Matera and K. Reuter, *Phys. Rev. B: Condens. Matter Mater. Phys.*, 2010, **82**, 085446.
- 34 S. Matera, M. Maestri, A. Cuoci and K. Reuter, *ACS Catal.*, 2014, **4**, 4081–4092.
- 35 R. Van de Vijver, B. R. Devocht, K. M. Van Geem, J. W. Thybaut and G. B. Marin, *Curr. Opin. Chem. Eng.*, 2016, **13**, 142–149.
- 36 M. Maestri, D. Livio, A. Beretta and G. Groppi, *Ind. Eng. Chem. Res.*, 2014, **53**, 10914–10928.
- 37 M. Maestri, D. G. Vlachos, A. Beretta, P. Forzatti, G. Groppi and E. Tronconi, *Top. Catal.*, 2009, **52**, 1983–1988.
- 38 M. Maestri and K. Reuter, *Chem. Eng. Sci.*, 2012, **74**, 296–299.
- 39 M. Maestri, in *New Strategies in Chemical Synthesis and Catalysis*, ed. B. Pignataro, Wiley-VCH, Weinheim, 2012, ch. 10, pp. 219–246.
- 40 C. T. Campbell, *J. Catal.*, 2001, **204**, 520–524.
- 41 A. Donazzi, A. Beretta, G. Groppi and P. Forzatti, *J. Catal.*, 2008, **255**, 241–258.
- 42 A. Donazzi, A. Beretta, G. Groppi and P. Forzatti, *J. Catal.*, 2008, **255**, 259–268.
- 43 A. Donazzi, M. Maestri, B. Micheal, A. Beretta, P. Forzatti, G. Groppi, E. Tronconi, L. D. Schmidt and D. G. Vlachos, *J. Catal.*, 2010, **275**, 270–279.



44 L. Dietz, S. Piccinin and M. Maestri, *J. Phys. Chem. C*, 2015, **119**, 4959–4966.

45 A. Beretta, G. Groppi, M. Lualdi, I. Tavazzi and P. Forzatti, *Ind. Eng. Chem. Res.*, 2009, **48**, 3825–3836.

46 N. Musselwhite and G. A. Somorjai, *Top. Catal.*, 2013, **56**, 1277–1283.

47 T. Bera, J. W. Thybaut and G. B. Marin, *ACS Catal.*, 2012, **2**, 1305–1318.

48 H. Stotz, L. Maier and O. Deutschmann, *Top. Catal.*, 2017, **60**, 83–109.

49 A. B. Mhadeshwar and D. G. Vlachos, *J. Phys. Chem. B*, 2005, **109**, 16819–16835.

50 H. Barron, G. Opletal, R. D. Tilley and A. S. Barnard, *Catal. Sci. Technol.*, 2016, **6**, 144–151.

51 J. Zhu, M. L. Yang, Y. D. Yu, Y. A. Zhu, Z. J. Sui, X. G. Zhou, A. Holmen and D. Chen, *ACS Catal.*, 2015, **5**, 6310–6319.

52 J. Yang, V. Froseth, D. Chen and A. Holmen, *Surf. Sci.*, 2016, **648**, 67–73.

53 Z. Ding, S. Guffanti and M. Maestri, unpublished material.

54 A. Maghsoumi, A. Ravanelli, F. Consonni, F. Nanni, A. Lucotti, M. Tommasini, A. Donazzi and M. Maestri, *React. Chem. Eng.*, submitted.

55 T. Avanesian, S. Dai, M. J. Kale, G. W. Graham, X. Q. Pan and P. Christopher, *J. Am. Chem. Soc.*, 2017, **139**, 4551–4558.

56 M. J. Kale and P. Christopher, *ACS Catal.*, 2016, **6**, 5599–5609.

57 J. C. Matsubu, S. Y. Zhang, L. DeRita, N. S. Marinkovic, J. G. G. Chen, G. W. Graham, X. Q. Pan and P. Christopher, *Nat. Chem.*, 2017, **9**, 120–127.

